Burns & Trauma, 2022, 10, tkac021
https://doi.org/10.1093/burnst/tkac021
Technical Report

OXFORD

Technical Report

LUtarjet-limit unique coracoid osteotomy Latarjet (With video)

Zhenhan Deng, Zeling Long and Wei Lu*

Department of Sports Medicine, The First Affiliated Hospital of Shenzhen University, Shenzhen Second People's Hospital, Shenzhen, Guangdong, 518035, China

*Correspondence. Email: weilu9309@gmail.com

Received 24 December 2021; Revised 10 March 2022; Editorial decision 12 April 2022

Abstract

Background: The Latarjet procedure is an effective technique for the treatment of recurrent anterior shoulder dislocation with glenoid bone loss. However, the inevitable destruction of the coracoacromial arch may result in humeral head translation. The aim of the study is to introduce a modified Latarjet technique with coracoacromial arch preservation as well as its short term clinical outcomes.

Methods: We propose a novel individualized flexible arthroscopic suture button fixation Latarjet technique called 'LUtarjet' with video. Precise measurements of the coracoid process, glenoid deficiency and osteotomy plane were made preoperatively. Only three arthroscopic portals were needed and limit unique coracoid osteotomy was performed with coracoacromial arch preservation. The mini window splitting of the subscapularis was performed from the posterior to the anterior direction and the split window was as small as 8–10 mm in length.

Results: A total of 27 patients (25.6 ± 5.4 years) were included in the study. The average surgical duration was 55.6 ± 6.3 min and the mean follow-up time was 8.1 ± 1.5 months. The functional score was significantly improved at the last follow-up. Radiologic evidence showed that the bone graft healing was placed in the desired position. No complications were found.

Conclusions: We present a fast, easy, accurate, safe arthroscopic 'LUtarjet' technique called FEAST that can simplify the arthroscopic Latarjet process and achieve a satisfactory bone graft position and satisfactory short-term clinical outcomes.

Level of evidence: IV, case series.

Key words: Latarjet, Recurrent anterior shoulder dislocation, Glenoid bone loss, Suture button fixation, Coracoacromial archBackground

Highlights

- This study is the first to examine the possibility of performing a flexible arthroscopic suture button fixation Latarjet procedure with coracoacromial arch preservation.
- This study is the first to show that the Limit Unique Coracoid Osteotomy Latarjet is able to simplify the Latarjet procedure process, achieve satisfactory bone graft position and provide promising clinical outcomes.

Background

In 1954, Latarjet first proposed the coracoid process (CP) transfer Latarjet operation for the treatment of refractory recurrent anterior dislocation of the shoulder joint [1] which was later popularized by Walch [2–4]. This technique reconstructed the anterior glenoid deficiency (static bone effect) and strengthened the anterior significantly weakened joint capsule and glenohumeral ligament (sling effect) [5,6]. Since

© The Author(s) 2020. Published by Oxford University Press.
This is an Open Access article distributed under the terms of the Creative Commons Attribution-NonCommercial License (https://creativecommons.org/licenses/by-nc/4.0/), which permits non-commercial re-use, distribution, and reproduction in any medium, provided the original work is properly cited. For commercial re-use, please contact journals.permissions@oup.com

Downloaded from academic.oup.com/burnstrauma/article/doi/10.1093/burnst/tkac021/6594419 by guest on 14 October 2026

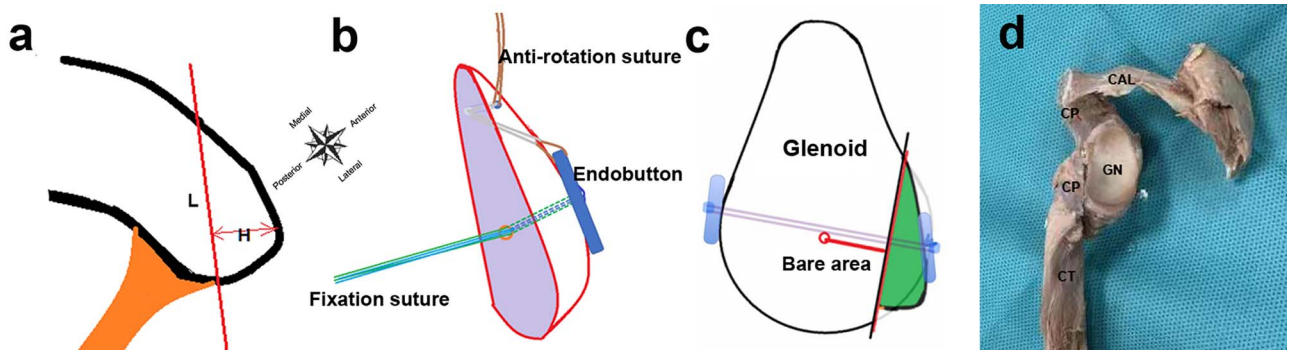

Figure 1. Schematic animation of the surgery. (**a**) The height and length of limit unique coracoid osteotomy can be individualized according to the size of the glenoid defect arc. (H, Height of the limit unique coracoid osteotomy; L, length of the limit unique coracoid osteotomy). (**b**) Coracoid bone block with anti-rotation and fixation bone tunnels and sutures. (**c**) The coracoid process is transferred, passed through the subscapularis and fixed on the anterior neck of the scapula with two cortical buttons and a 4-strand suture. (**d**) Schematic diagram of the principle of surgery on a cadaveric specimen. *CAL* Coracoacromial ligament, *CP* coracoid process, *CT* conjoined tendon, *GN* glenoid

the invention of the Latarjet procedure, the postoperative recurrence rate of refractory recurrent dislocation of the shoulder joint has been significantly reduced and the return-to-sports rate and patient satisfaction have been greatly improved [7–11]. With the improvement of arthroscopic technology, Laffose *et al*. first tried arthroscopic Latarjet and achieved great success [12,13]. Boileau's modified arthroscopic flexible fixation of Latarjet has further improved the technique, which effectively avoids the complications of screw fixation [14–16]. The bone block positioning was more accurate and controlled and the clinical outcomes were also excellent. Our middle-term follow-up of the modified suture-button fixation technique found not only that the graft absorbs less but also that the graft tends to expand and remodel to the formation of an outer fitting circle (OFC) similar to the healthy side glenoid over time [17,18].

However, both the screw and flexible fixation Latarjet procedures will inevitably cause coracoacromial arch (CAA) destruction and scapular abnormalities, which have been criticized by scholars [19–22]. One concern is the increased risk of superior translation of the humeral head without CAA shielding, especially in patients with massive rotator cuff tears [23–27]. To the best of our knowledge, there are currently no reports on the Latarjet technique with CAA preservation. In this study, we propose a novel individualized flexible arthroscopic suture button fixation Latarjet technique (called 'LUtarjet', named after Dr Wei Lu, the designer and chief surgeon of the technique) with limit unique coracoid osteotomy, mini window splitting of the subscapularis and CAA preservation (Figure 1).

Methods

Patient selection

This study was approved by the Ethical Committee of Shenzhen Second People's Hospital (20210722001-FS02) and all patients gave informed consent for the operation before surgery. The patients who underwent the individualized flexible fixation Latarjet procedure were included in the study. Glenoid bone loss (GBL) measurement was based on a preoperative computed tomography (CT) scan. The inclusion criteria were as follows: (1) 20% < GBL < 25%; (2) 15% < GBL < 20% + instability severity index score (ISIS) score > 6 and 10% < GBL < 15% + competitive sports level; (3) revision. Patients with no or minimal GBL and those with epilepsy and obvious osteoporosis were excluded.

Preoperative design

3D CT reconstruction was performed to outline the CP of the bilateral shoulder joints preoperatively. The optimal glenoid OFC of the healthy side should be determined on the en face view and mirrored to the affected side. The proportion of GBL and the size and shape of the defect arc on the affected side should be measured based on the glenoid of the healthy side (Figure 2a, b). The length, width and thickness of the CP were measured on 2D CT images and the preoperative design of the CP osteotomy level was made in each case (Figure 2c). The bone block can be designed from the CP according to the size and shape of the glenoid defect arc (GDA). Generally, when the GBL is 20%, the GDA is 5–6 mm wide and the arc length is 15–18 mm. Due to the possibility of early bone absorption after the Latarjet procedure, the bone block should have a width of 6–8 mm and an arc length of 15–18 mm from the CP (10% larger than the defect).

Surgical procedures

The surgical technique was modified primarily on the basis of a previously described technique (Video) [17,18]. The procedure was performed under general anesthesia associated with an interscalenic block with the patient in the beach chair position. The upper limb was placed in the neutral position with a Spider Limb Positioner (Smith & Nephew, USA) without any traction. Only one incision and three portals are needed to complete the whole procedure (Figure 2d).

Step 1. Limit unique coracoid osteotomy and bone block preparations A straight incision 25 mm inferior to the tip of the CP was made. The deltoid muscle was separated and then

Downloaded from academic.oup.com/burnstrauma/article/doi/10.1093/burnst/tkac021/6594419 by guest on 14 October 2026

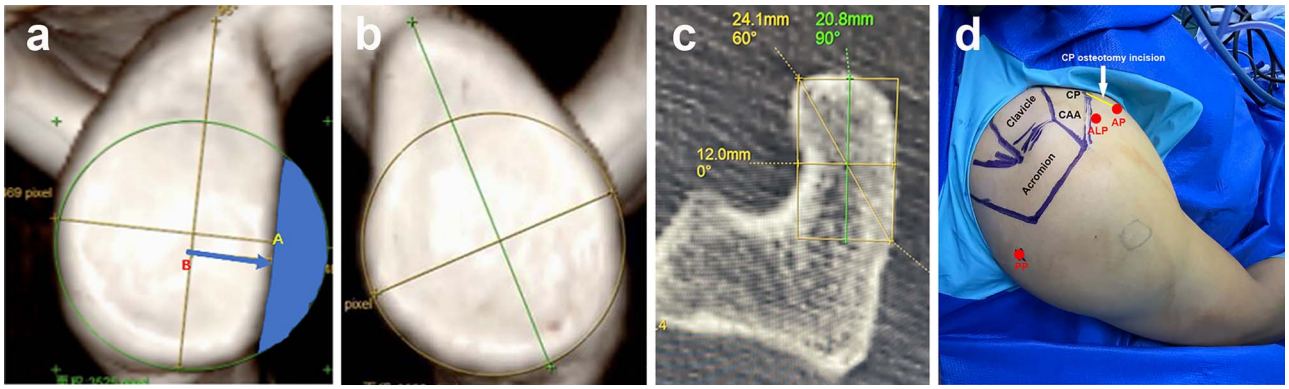

Figure 2. Preoperative measurement and design. (**a**) Injury side glenoid with GBL. The blue area represents the glenoid defect arc. Circles represent the optimal outer fitting circle (OFC). (**b**) Normal side glenoid. Circles represent the optimal OFC. (**c**) Measurements of length, width and thickness of the coracoid process and design of the limit unique coracoid osteotomy plane. (**d**) Surgical approaches in a right shoulder. *AP* Anterior portal, *ALP* anterolateral portal, *PP* posterior portal, *GBL* glenoid bone loss

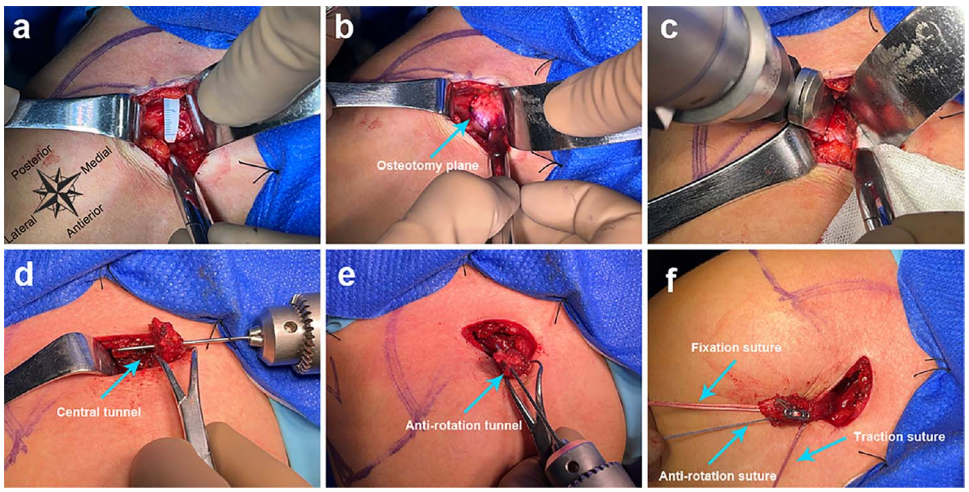

Figure 3. Limit unique coracoid osteotomy and bone block preparations. (**a**) Measurement of the coracoid process. (**b**) Marking of the limit unique coracoid osteotomy plane. (**c**) Limit unique coracoid osteotomy using an oscillating saw. (**d**) Central tunnel creation. (**e**) Anti-rotation tunnel creation. (**f**) Bone block preparation with sutures

the CP was exposed. Once insertion of the coracoacromial ligament (CAL) and pectoralis minor on the CP was achieved, the pectoralis minor fibers were separated from the bone inward on the medial side of the CP by radiofrequency (RF) and insertion of the lateral CAL was carried out. An oscillating saw was used to cut the bone downward along the designed line. The coracoid bone block is usually a triangular block $15 \times 8 \times 10$ mm in length, width and height, respectively, which does not need to be decorticated (Figure 3a–c). The bone block was grasped and turned over with the cutoff surface facing upward. After trimming with a bone rongeur, the bone block was placed outside the incision. The whole conjoint tendon was intact and was separated downward using the index finger until the conjoint tendon pedicle was 5 cm long to ensure that the bone block could easily fit with the glenoid without tension.

A 2.5 mm central tunnel (C tunnel) was perpendicularly made in the center of the osteotomy plane. An EndoButton (Smith & Nephew, USA) was placed on the other side (Figure 3d). Three high-strength sutures (DePuy Mitek, USA) were put through the EndoButton and coracoid bone tunnels for later use. A 1.5 mm anti-rotation tunnel (A tunnel), perpendicular to the C tunnel and for passage of an anti-rotation suture, was drilled from inside to outside parallel to the surface 3 mm away from the distal end of the bone block (Figure 3e). A high-strength suture for antirotation was pulled through the Endobutton's side hole and then through the A tunnel for later use. The outlet of the anti-rotation suture was placed on the lateral side of the bone block (Figure 1b). If necessary, a traction suture can be placed at the junction of the conjoint tendon and the CP to prevent accidental intraoperative suture winding (Figure 3f). Upon completion of the settings, all the preset sutures on the CP, except the antirotation suture, were placed into the cannula and then into the incision behind the pectoralis major and in front of the subscapularis. Then, this incision was closed to avoid water leakage and to improve the view and was used as the anterior portal (A portal).

Downloaded from academic.oup.com/burnstrauma/article/doi/10.1093/burnst/tkac021/6594419 by guest on 14 October 2026

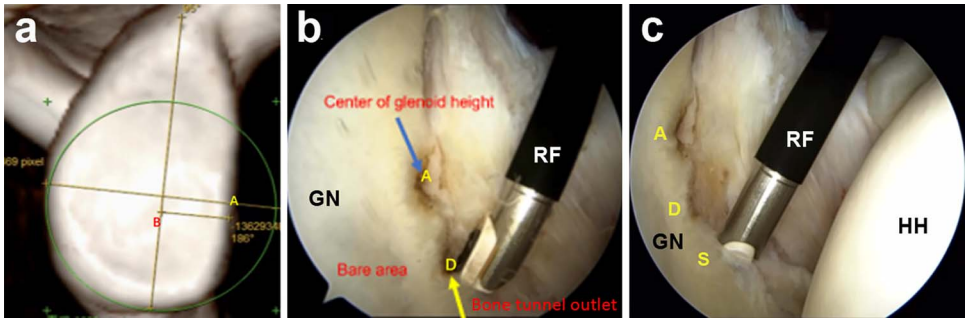

Figure 4. Localization of glenoid deficit arc, bone tunnel and anti-rotation anchor, and the plane of subscapularis split. (**a**) Location in 3D computed tomography en face view. (**b**) Anterior glenoid under arthroscopy. The blue arrow shows the center of the glenoid height. The yellow arrow shows the bone tunnel outlet. (**c**) Plane of subscapularis split. *A* Anti-rotation anchor positioning, *D* projection position of bone tunnel outlet, *GN* glenoid, *HH* humeral head, *RF* radiofrequency, *S* split subscapularis plane

Step 2. Glenoid preparation, bone tunnel positioning and drilling After creation of the posterior portal (P portal) and anterolateral portal (AL portal), arthroscopic examination was performed throughout the joint, especially for GBL, Hill–Sachs and other lesions. The rotator cuff interval tissue was cleaned off to expose the front CP and the posterior edge of the pectoralis major. Viewing from the P portal, the midpoint of the anterior glenoid edge was marked as point A, which is the position of the anti-rotation anchor insertion (Figure 4a). The bare area of the glenoid was observed and used as the reference for glenoid bone tunnel drilling. If there is no detection of a bare area, A point can be used as the reference. The extension point in front of the bare area is the outlet of the glenoid bone tunnel, which is marked as point D, located at the midpoint of the GDA. If it is difficult to determine the center of the OFC, the midpoint between the upper edge of the subscapular tendon and the lower edge of the glenoid defect is marked as RF (used as the bone tunnel drill point; yellow arrow in Figure 4b). The plane of the subscapularis split was 5 mm below the extension line in front of the bare area, equivalent to 5 o'clock, lower than the bone tunnel centered on the bare area (Figure 4c).

An arthroscope was placed into the AL portal to observe and freshen the glenoid deficiency bed. The bare area of the glenoid or the center of the OFC before the operation was observed and served as a reference for the positioning of the bone tunnel and the center of the bone block. A prepositioning drill was placed on the preset bone tunnel with an arthroscopic microfracture awl (Figure 5a). A self-designed bone tunnel locator was inserted along the switch stick, and the guiding needle was inserted. After expanding the tunnel with a 4.5 mm drill, a polydioxanone (PDS) suture was inserted as the guide suture for bone block high-strength suture pulling (Figure 5b, c). Viewing from the AL portal, the split window in front of the subscapularis was visualized and its relationship with the axillary nerve was observed (Figure 5d). We found that in ~50% of cases, when the shoulder joint is in the neutral position, the axillary nerve is inferior and far medial to the split window, while it is difficult to visualize in the other 50% of cases. As the soft tissue around the nerve will protect it from interference, it is unnecessary to perform massive subscapularis separation.

Step 3. Mini window splitting of subscapularis The shoulder joint was placed in the neutral position. The subscapularis was split by RF from posterior to anterior (Figure 6a). The medial border of the split window is the glenoid surface and the lateral border is the humeral head plane. The muscle membrane behind the subscapularis on the glenoid plane was split until its front side can be clearly visualized (Figure 6b). Then, the switch stick passed through the split window from anterior to posterior through the A portal and the subscapularis was pushed aside superomedially. RF was introduced into the AL portal and the split window was further split laterally by 8–10 mm at its front (Figure 6c).

Step 4. Bone block transfer and fixation A suture retriever was inserted from the A portal, running through the canal with the high-strength suture inside, then in front of the subscapularis and through the split window under direct vision, thus retrieving the guide suture of the glenoid bone tunnel from the canal. Then, the high-strength suture was pulled into the bone tunnel by the guide suture and pulled out from the rear P portal (Figure 7a). After the posture of the bone block was adjusted perpendicular to the split window, the anti-rotation suture in the front was caught by a suture retriever passing from the window of the subscapularis through the P portal and pulled to the rear. At the same time, fixation sutures and anti-rotation sutures were pulled in turn to pull the bone block entirely into the glenohumeral joint through the subscapularis (Figure 7b, c). Then, the anti-rotation suture was pulled out from the L portal. The use of the anti-rotation suture allows matching of the osteotomy surface of the bone block to the glenoid rim, adjusting the bone graft so it is flush to or slightly elevated compared to the glenoid surface (Figure 7d). A Tennessee knot was tied at the rear. The anti-rotation suture was fixed at the preset A point at the anterior edge of the glenoid with a PushLock anchor (Arthrex, USA) (Figure 7e, f). The shoulder joint was rotated to observe the stability of the bone block. The capsule does

Downloaded from academic.oup.com/burnstrauma/article/doi/10.1093/burnst/tkac021/6594419 by guest on 14 October 2026

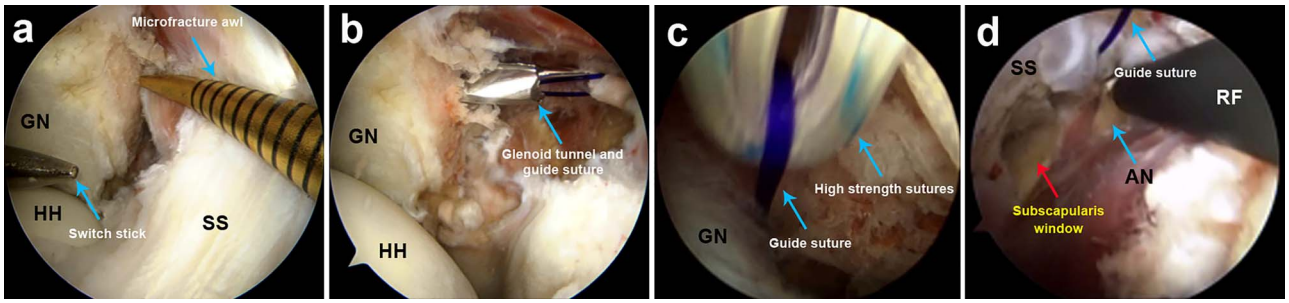

Figure 5. Bone tunnel positioning and drilling. (**a**) A microfracture awl marking the outlet of the bone tunnel. (**b**) Guide suture placement. (**c**) Polydioxanone suture guidance of the high-strength suture from the bone block passing the bone tunnel. (**d**) Anatomical relationship among the subscapularis split window, axillary nerve and guide suture. *GN* Glenoid, *RF* radiofrequency, *SS* subscapularis, *HH* humeral head

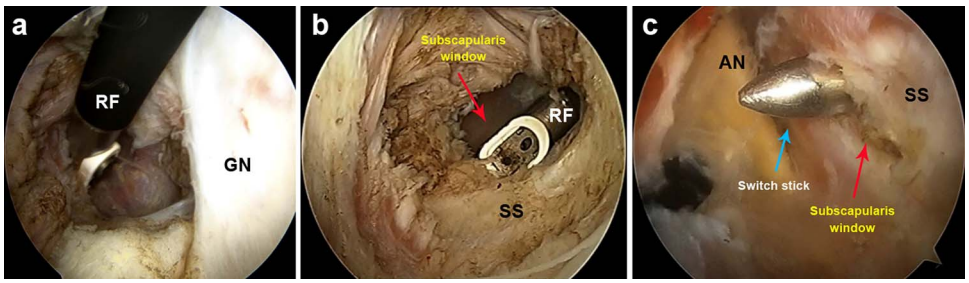

Figure 6. Mini window splitting of the subscapularis. (**a**) Visualizing the muscular membrane in front of the subscapularis. (**b**) Splitting the subscapularis window laterally ~8–10 mm. (**c**) Anterior view of the subscapularis split window and axillary nerve. *AN* Axillary nerve, *GN* glenoid, *RF* radiofrequency, *SS* subscapularis

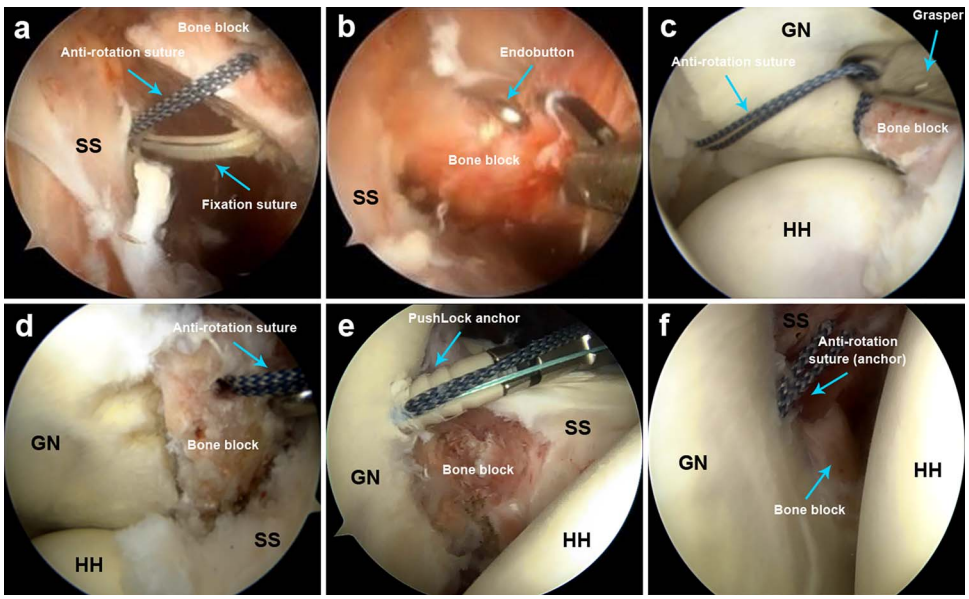

Figure 7. Bone block transfer and fixation. (**a**) The fixation suture and anti-rotation suture were pulled to the rear and the bone block was placed in front of the subscapularis. (**b**) The bone block and subscapularis split window were adjusted to the vertical position. (**c**) The bone block was pulled into the glenohumeral joint. (**d**) The anti-rotation line was adjusted to flush the bone block to the glenoid articular surface. (**e**) A knotless suture anchor was fixed to the glenoid to prevent rotation of the bone block. (**f**) The bone block was fixed to the glenoid. *GN* Glenoid, *RF* radiofrequency, *SS* subscapularis, *HH* humeral head

not need to be sutured to prevent external rotation limitation of the shoulder joint after the operation [18,28].

Postoperative rehabilitation

The arm was immobilized for 6 weeks in a neutral rotation sling. Because the fixation is strong, upper limb activity within its capacity was allowed, including pendulum exercise (five times a day, 5 min each session). After 6 weeks, the sling was removed and formal rehabilitation with a physiotherapist was started. A return to everyday life was encouraged. No heavy repeated lifting was allowed for the first 6 months to avoid postoperative bone absorption caused by strong pulling of the biceps. Return to all types of sports activities,

Downloaded from academic.oup.com/burnstrauma/article/doi/10.1093/burnst/tkac021/6594419 by guest on 14 October 2026

including collision and contact-overhead sports, was allowed 12 months postoperatively.

Evaluation of clinical efficacy

Radiography and 3D CT were performed routinely for the preoperative evaluation ofglenoid and humeral bone defects. The patients were routinely required to undergo a radiological examination at 3, 6 and 12 months after the operation. The Rowe score and Walch–Duplay score were used for clinical assessment. Meanwhile, complications that occurred intraoperatively and postoperatively were recorded and the occurrence rate was calculated.

Statistical analysis

Statistical analysis was conducted using SPSS Version 16.0 software (IBM Corp). Pairwise comparisons were performed using a paired t test, and $p < 0.05$ was considered statistically significant.

Results

A total of 27 patients were included in the study, comprising 23 males and 4 females with a mean age of 25.6 ± 5.4 years. The average surgical duration was 55.6 ± 6.3 min and the mean follow-up time was 8.1 ± 1.5 months.

At the last follow-up, the Rowe score and Walch–Duplay scores of the patients increased from 40.5 ± 7.0 and 57.9 ± 10.8 preoperatively to 93.7 ± 4.1 and 95.1 ± 5.3 postoperatively, respectively ($p < 0.05$). Postoperative magnetic resonance imaging (MRI) showed the integrity of the CAL, indicating preservation of the CAA (Figure 8). A 3D CT scan showed bone graft healing in the desired position after the operation (Figure 9). There was only one case of soft union due to excessive exercise. No recurrent dislocation, positive apprehension sign, postoperative infection, axillary nerve injury or vascular injury occurred in any patient.

Discussion

The Latarjet procedure, first proposed in 1954, created a new era in the treatment and research of recurrent shoulder dislocation [1]. In 2012, Boileau's modified flexible fixation technique greatly reduced the screw-related complications of the traditional Latarjet procedure, making the placement of the bone block more accurate and controlled and increasing the healing rate of the graft [7,14,16]. Our study found that graft expanding remodeling after flexible fixation Latarjet provided excellent clinical outcomes [17,18]. However, the inherent disadvantages of the Latarjet procedure, such as the destruction of the CAA and obvious interference with the subscapularis, have been criticized [19,21,22,25].

Flexible fixation of the Latarjet procedure was first proposed by Boileau. This method does not require a large volume of CP and overcomes the shortcomings of the traditional Latarjet procedure, such as the complications of fixed grafts, large deviations in bone block positioning and excessive bone resorption [29–34]. According to our previous research on the remodeling characteristics of bone blocks after flexible fixation Latarjet [17,18], we proposed the concept of GDA of recurrent dislocation of the shoulder joint and designed a modified flexible fixation Latarjet technique with individualized limit unique coracoid osteotomy according to the size and shape of the glenoid defect and preservation of the CAA.

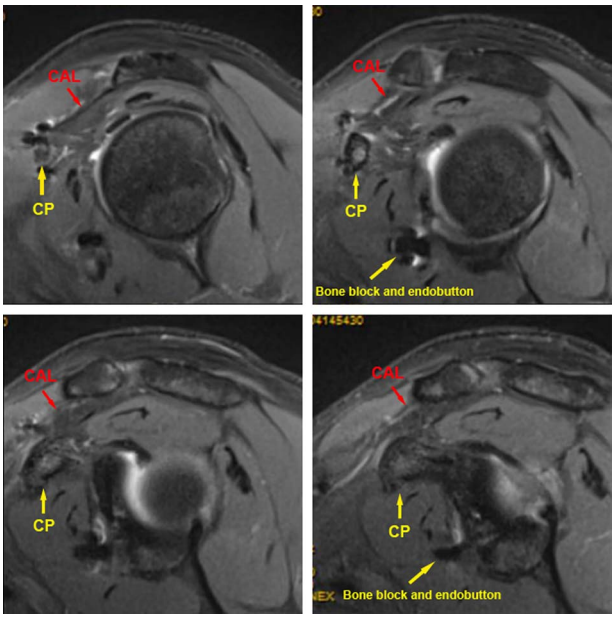

Figure 8. Postoperative MRI shows the integrity of the CAL, indicating preservation of the coracoacromial arch. *CAL* Coracoacromial ligament, *CP* coracoid process, *MRI* magnetic resonance imaging

Theoretically, this idea can be understood based on the following observations. First, in traditional Latarjet, the bone block must be large enough to accommodate two screws, so limit unique coracoid osteotomy is impossible. However, the flexible fixation Latarjet procedure does not have a high demand for a large graft and part of the coracoid bone block is sufficient in mass for use as an ideal graft with easy fixation. Second, the flexible fixation Latarjet procedure has less bone absorption and the bone block in most cases will be remodeled and expanded. Therefore, the size of the CP that is intercepted can be individually designed to be slightly larger than the defect (usually 20%). According to 25% GBL equals an approximately 5 mm deficiency of OFC diameter, and the according width of limit osteotomy is more than 6 mm. The mean length, width and height of the CP were 45.2 ± 4.1, 24.9 ± 2.5 and 11.9 ± 1.8 mm, respectively [35]. Therefore, the CP is usually large enough to serve as the graft. The length of the bottom surface of the CP attached to the glenoid of limit unique coracoid osteotomy can be individualized according to the length of the GDA. In addition, because the proportion of limit unique coracoid osteotomy is less than one-quarter of the whole CP and the bottom of the residual coracoid process is a wide triangle, there is no concern about residual CP fracture [36,37]. Last

Downloaded from academic.oup.com/burnstrauma/article/doi/10.1093/burnst/tkac021/6594419 by guest on 14 October 2026

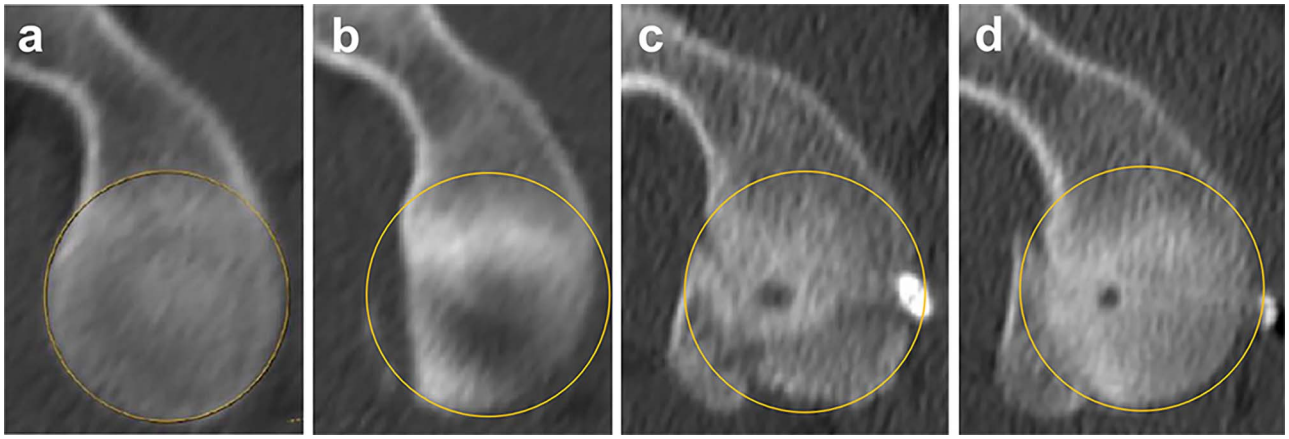

Figure 9. Computed tomography images of one representative case that underwent the individualized flexible fixation Latarjet procedure (en face view of the glenoid). (**a**) Preoperative mirror image of the normal side. (**b**) Injury side with glenoid bone loss preoperatively. (**c**) Injury side immediately after surgery. (**d**) Injury side at 6 months after surgery. The circle indicates the outer fitting circle

but not least, the plane of limit unique coracoid osteotomy can be designed beforehand according to the size and shape of the GDA on 3D CT reconstruction and can simulate transfer of the graft to the defective glenoid to form the OFC.

This modification has the following advantages: (1) Fast. The entire operation can be completed within 60 min, which makes it worth popularizing. (2) Easy. Open surgery of limit unique coracoid osteotomy and bone block preparations can be conducted without arthroscopic illusion and a long learning curve. The coracoid bone block does not need to be decorticated and the osteotomy is simpler. Only three arthroscopic portals are needed. Although the subscapularis split window is small, it is relatively simple to pass through the subscapularis because the bone block is small and triangle-shaped with a small front and a large back. (3) Accurate. Open surgery for limit unique coracoid osteotomy and bone block preparations, including bone tunnel drilling and suture placement, is more accurate. The glenoid bone canal can be precisely positioned at 4 o'clock on the right shoulder or 8 o'clock on the left shoulder by using the self-designed bone tunnel locator. (4) Safe. Quantification of the osteotomy can be performed from the CP, thereby preserving the CAA and avoiding possible complications arising therefrom in the future. Limit unique coracoid osteotomy under direct vision can protect against musculocutaneous nerve injury. To the best of our knowledge, the 8–10 mm split window of the subscapularis is the most minimally invasive incision reported in the literature (usually 20 mm) [12,38]. Due to the small interference (<10 mm) to the subscapularis, all splits are located laterally to the glenoid surface without involving the axillary nerve, which is medial to the glenoid. In addition, due to the preservation of the surrounding soft tissue of the axillary nerve, interference with the axillary nerve during the whole operation is minimized. In brief, this is a fast, easy, accurate and safe technique, which is referred to as FEAST.

The axillary nerve originates from the posterior bundle of the brachial plexus, running along the upper medial part of the subscapular tendon and passing its front surface, and enters the quadrilateral foramen laterally and posteriorly [39,40]. According to the literature, the average distance from the anterior projection point of the subscapular tendon at the glenoid 3–5 o'clock position to the axillary nerve was 18.2 ± 8.1 (15–28) mm [40–42]. In our experience, after a modified small splitting in the subscapular tendon, when we observed from the A portal, the axillary nerve was located medial to the split window and to the glenoid surface. In this procedure, subscapularis splitting is performed laterally to the glenoid surface and separated by a switch stick with a direct view. The RF for splitting enters from the portal AL, which is perpendicular to the axillary nerve, and the chance of RF damaging the axillary nerve is very low.

In traditional Latarjet, due to the relatively high proportion of bone resorption and the need for two screws, a large bone block must be cut for better fixation. In our flexible fixation Latarjet procedure with whole coracoid osteotomy, mid-term results have demonstrated bone block expansion remodeling, in which the defective glenoid tends to restore the OFC of the original glenoid, and the grafts outside the circle are absorbed [18]. This new technique is an improvement based on our previous method; only a small bone tunnel is needed and limit unique coracoid osteotomy was designed similarly to the GDA and achieved good short-term clinical outcomes. Iliac crest bone graft transfer and remplissage is considered a salvage procedure in case the surgery fails. Flexible fixation also presents several drawbacks, one of which is inadequate fixation strength. In addition, the upper limb immobilization time is generally 3 months, which is slightly longer than that of other surgical methods. Graft absorption occurred in a few cases, mostly due to excessive exercise. Future studies will be carried out to report the long-term clinical outcome and reveal the underlying mechanism.

Downloaded from academic.oup.com/burnstrauma/article/doi/10.1093/burnst/tkac021/6594419 by guest on 14 October 2026

Conclusions

This individualized flexible fixation Latarjet procedure consists of limit unique coracoid osteotomy, mini window-splitting of subscapularis and CAA preservation, and can simplify the Latarjet process while achieving a better graft position and healing and satisfactory short-term clinical outcomes. It has good repeatability with a shortened learning curve, and the expected effect of FEAST can be achieved.

Abbreviations

A portal: Anterior portal; A tunnel: Antirotation tunnel; AL portal: Anterolateral portal; C tunnel: Central tunnel; CAA: Coracoacromial arch; CAL: Coracoacromial ligament; CP: Coracoid process; CT: Computed tomography; FEAST: Fast, easy, accurate and safe technique; GBL: Glenoid bone loss; GDA: Glenoid defect arc; ISIS: Instability severity index score; OFC: Outer fitting circle; P portal: Posterior portal; PDS: Polydioxanone; RF: Radiofrequency.

Supplementary data

Supplementary data is available at *Burns & Trauma Journal* online.

Funding

This study was supported by the National Natural Science Foundation of China (81902303), Guangdong Basic and Applied Basic Research Foundation (2021A1515220030, 2020A151501048), Shenzhen Science and Technology Program (RCYX20210609103902019, RCBS20200714114856299, JCYJ20190806164216661) and Clinical Research Project of Shenzhen Second People's Hospital (20203357028, 20213357011, 20203357034, GK202203008).

Authors' contributions

ZD contributed to the conceptual design of the study, collected and analysed the data, drafted the manuscript, interpreted the data and provided funding support. ZL contributed to video editing and literature research. WL contributed to the conceptual design of the study, performed the surgery and provided funding support. All authors have given final approval and agree to be accountable for all aspects of the work.

Ethics approval and consent to participate

Shenzhen Second People's Hospital Institutional Review Board approved this study (20210722001-FS02).

Consent for publication

All authors agree with the submission of this article to *Burns & Trauma*.

Conflicts of interest

None declared.

Data availability

The datasets used and/or analysed in the current study are available from the corresponding author upon reasonable request.

References

1. Latarjet M. Treatment of recurrent dislocation of the shoulder. *Lyon Chir*. 1954;49:994–7.
2. Walch G, Charret P, Pietro-Paoli H, Dejour H. Anterior recurrent luxation of the shoulder. Postoperative recurrences. *Rev Chir Orthop Reparatrice Appar Mot*. 1986;72:541–55.
3. Young AA, Maia R, Berhouet J, Walch G. Open Latarjet procedure for management of bone loss in anterior instability of the glenohumeral joint. *J Shoulder Elb Surg*. 2011;20:S61–9. https://doi.org/10.1016/j.jse.2010.07.022.
4. Joshi MA, Young AA, Balestro JC, Walch G. The Latarjet-Patte procedure for recurrent anterior shoulder instability in contact athletes. *Clin Sports Med*. 2013;32:731–9.
5. Giles JW, Boons HW, Elkinson I, Faber KJ, Ferreira LM, Johnson JA, *et al*. Does the dynamic sling effect of the Latarjet procedure improve shoulder stability? A biomechanical evaluation. *J Shoulder Elb Surg*. 2013;22:821–7.
6. Yamamoto N, Muraki T, An KN, Sperling JW, Cofield RH, Itoi E, *et al*. The stabilizing mechanism of the Latarjet procedure: a cadaveric study. *J Bone Joint Surg Am*. 2013;95:1390–7.
7. Bhatia S, Frank RM, Ghodadra NS, Hsu AR, Romeo AA, Bach BR, Jr, *et al*. The outcomes and surgical techniques of the latarjet procedure. *Art Ther*. 2014;30:227–35.
8. Schmid SL, Farshad M, Catanzaro S, Gerber C. The Latarjet procedure for the treatment of recurrence of anterior instability of the shoulder after operative repair: a retrospective case series of forty-nine consecutive patients. *J Bone Joint Surg Am*. 2012;94:e75. https://doi.org/10.2106/JBJS.K.00380.
9. Hardy A, Sabatier V, Laboudie P, Schoch B, Nourissat G, Valenti P, *et al*. Outcomes after Latarjet procedure: patients with first-time versus recurrent dislocations. *Am J Sports Med*. 2020;48:21–6.
10. Hurley ET, Jamal MS, Ali ZS, Montgomery C, Pauzenberger L, Mullett H. Long-term outcomes of the Latarjet procedure for anterior shoulder instability: a systematic review of studies at 10-year follow-up. *J Shoulder Elb Surg*. 2019;28:e33–9. https://doi.org/10.1016/j.jse.2018.08.028.
11. Rollick NC, Ono Y, Kurji HM, Nelson AA, Boorman RS, Thornton GM, *et al*. Long-term outcomes of the Bankart and Latarjet repairs: a systematic review. *Open Access J Sports Med*. 2017;8:97–105.
12. Lafosse L, Lejeune E, Bouchard A, Kakuda C, Gobezie R, Kochhar T. The arthroscopic Latarjet procedure for the treatment of anterior shoulder instability. *Art Ther*. 2007;23:e1241–5. https://doi.org/10.1016/j.arthro.2007.06.008.
13. Lafosse L, Boyle S, Gutierrez-Aramberri M, Shah A, Meller R. Arthroscopic latarjet procedure. *Orthop Clin North Am*. 2010;41:393–405.
14. Boileau P, Gendre P, Baba M, Thélu CÉ, Baring T, Gonzalez JF, *et al*. A guided surgical approach and novel fixation

Downloaded from academic.oup.com/burnstrauma/article/doi/10.1093/burnst/tkac021/6594419 by guest on 14 October 2026

method for arthroscopic Latarjet. *J Shoulder Elb Surg*. 2016;25: 78–89.
15. Gendre P, Thélu CE, d'Ollonne T, Trojani C, Gonzalez JF, Boileau P. Coracoid bone block fixation with cortical buttons: An alternative to screw fixation? *Orthop Traumatol Surg Res*. 2016;102:983–7.
16. Boileau P, Saliken D, Gendre P, Seeto BL, d'Ollonne T, Gonzalez JF, *et al*. Arthroscopic Latarjet: suture-button fixation is a safe and reliable alternative to screw fixation. *Art Ther*. 2019;35:1050–61.
17. Xu J, Liu H, Lu W, Zhu W, Peng L, Ouyang K, *et al*. Clinical outcomes and radiologic assessment of a modified suture button arthroscopic Latarjet procedure. *BMC Musculoskelet Disord*. 2019;20:173.
18. Xu J, Liu H, Lu W, Deng Z, Zhu W, Peng L, *et al*. Modified arthroscopic Latarjet procedure: suture-button fixation achieves excellent Remodeling at 3-year follow-up. *Am J Sports Med*. 2020;48:39–47.
19. Lee TQ, Black AD, Tibone JE, McMahon PJ. Release of the coracoacromial ligament can lead to glenohumeral laxity: a biomechanical study. *J Shoulder Elb Surg*. 2001;10: 68–72.
20. Jacxsens M, Elhabian SY, Brady SE, Chalmers PN, Tashjian RZ, Henninger HB. Coracoacromial morphology: a contributor to recurrent traumatic anterior glenohumeral instability? *J Shoulder Elb Surg*. 2019;28:1316–25.e1. https://doi.org/10.1016/j.jse.2019.01.009.
21. Su WR, Budoff JE, Luo ZP. The effect of coracoacromial ligament excision and acromioplasty on superior and anterosuperior glenohumeral stability. *Art Ther*. 2009;25:13–8.
22. Wellmann M, Petersen W, Zantop T, Schanz S, Raschke MJ, Hurschler C. Effect of coracoacromial ligament resection on glenohumeral stability under active muscle loading in an in vitro model. *Art Ther*. 2008;24:1258–64.
23. Panni AS, Milano G, Lucania L, Fabbriciani C, Logroscino CA. Histological analysis of the coracoacromial arch: correlation between age-related changes and rotator cuff tears. *Art Ther*. 1996;12:531–40.
24. Boes MT, McCann PD, Dines DM. Diagnosis and management of massive rotator cuff tears: the surgeon's dilemma. *Instr Course Lect*. 2006;55:45–57.
25. Sakoma Y, Sano H, Shinozaski N, Itoigawa Y, Yamamoto N, Itoi E. Coverage of the humeral head by the coracoacromial arch: relationship with rotator cuff tears. *Acta Med Okayama*. 2013;67:377–83.
26. Soslowsky LJ, An CH, DeBano CM, Carpenter JE. Coracoacromial ligament: in situ load and viscoelastic properties in rotator cuff disease. *Clin Orthop Relat Res*. 1996;40-4.
27. Hansen ML, Otis JC, Johnson JS, Cordasco FA, Craig EV, Warren RF. Biomechanics of massive rotator cuff tears: implications for treatment. *J Bone Joint Surg Am*. 2008;90: 316–25.
28. Sahu D. Capsular repair is not an important part of the Latarjet-Walch procedure. *J Shoulder Elb Surg*. 2021;31:948–56.
29. Shah AA, Butler RB, Romanowski J, Goel D, Karadagli D, Warner JJ. Short-term complications of the Latarjet procedure. *J Bone Joint Surg Am*. 2012;94:495–501.
30. Giacomo GD, Costantini A, de Gasperis N, De Vita A, Lin BK, Francone M, *et al*. Coracoid bone graft osteolysis after Latarjet procedure: a comparison study between two screws standard technique vs mini-plate fixation. *Int J Shoulder Surg*. 2013;7:1–6.
31. Hurley ET, Schwartz LB, Mojica ES, Campbell KA, Matache BA, Meislin RJ, *et al*. Short-term complications of the Latarjet procedure: a systematic review. *J Shoulder Elb Surg*. 2021;30: 1693–9.
32. Athwal GS, Meislin R, Getz C, Weinstein D, Favorito P. Short-term complications of the arthroscopic Latarjet procedure: a north American experience. *Art Ther*. 2016;32:1965–70.
33. Frank RM, Gregory B, O'Brien M, Bernardoni E, Verma NN, Cole BJ, *et al*. Ninety-day complications following the Latarjet procedure. *J Shoulder Elb Surg*. 2019;28:88–94.
34. Cho CH, Na SS, Choi BC, Kim DH. Complications related to Latarjet shoulder stabilization: a systematic review. *Am J Sports Med*. 2021;3635465211042314. https://doi.org/10.1177/03635465211042314.
35. Rios CG, Arciero RA, Mazzocca AD. Anatomy of the clavicle and coracoid process for reconstruction of the coracoclavicular ligaments. *Am J Sports Med*. 2007;35:811–7.
36. Swan J, Boileau P, Barth J. Arthroscopic Trillat procedure: a guided technique. *Arthrosc Tech*. 2020;9:e513–9. https://doi.org/10.1016/j.eats.2019.12.004.
37. Mascarenhas R, Rusen J, Saltzman BM, Leiter J, Chahal J, Romeo AA, *et al*. Management of humeral and glenoid bone loss in recurrent glenohumeral instability. *Adv Orthop*. 2014;2014:640952. https://doi.org/10.1155/2014/640952.
38. Lafosse L, Boyle S. Arthroscopic Latarjet procedure. *J Shoulder Elb Surg*. 2010;19:2–12.
39. Wai CJ. Axillary anatomy and history. *Curr Probl Cancer*. 2012;36:234–44.
40. Simone JP, Streubel PN, Sanchez-Sotelo J, Steinmann SP, Adams JE. Change in the distance from the axillary nerve to the Glenohumeral joint with shoulder external rotation or abduction position. *Hand (N Y)*. 2017;12:395–400.
41. Hawi N, Reinhold A, Suero EM, Liodakis E, Przyklenk S, Brandes J, *et al*. The anatomic basis for the arthroscopic Latarjet procedure: a cadaveric study. *Am J Sports Med*. 2016;44:497–503.
42. Yoo JC, Kim JH, Ahn JH, Lee SH. Arthroscopic perspective of the axillary nerve in relation to the glenoid and arm position: a cadaveric study. *Art Ther*. 2007;23:1271–7.

Downloaded from academic.oup.com/burnstrauma/article/doi/10.1093/burnst/tkac021/6594419 by guest on 14 October 2026